

## Targeted delivery of bleomycin to the brain using photo-chemical internalization of *Clostridium perfringens* epsilon prototoxin

Henry Hirschberg · Michelle J. Zhang · H. Michael Gach ·  
Francisco A. Uzal · Qian Peng · Chung-Ho Sun ·  
David Chighvinadze · Steen J. Madsen

Received: 4 March 2009 / Accepted: 24 May 2009 / Published online: 9 June 2009  
© The Author(s) 2009. This article is published with open access at Springerlink.com

**Abstract** Cells infiltrating into normal brain from malignant brain tumors are protected by the blood brain barrier (BBB) which prevents the delivery and limits the effects of anti-tumor agents. We have evaluated the ability of photochemical internalization (PCI) to limit the effects of an agent known to broadly open the BBB to a target region of the brain. The PCI-based relocation and activation of macromolecules into the cell cytosol has the advantage of minimal side effects since the effect is localized to the area exposed to light, allowing the access of chemotherapeutic agents only to these regions. Non tumor bearing inbred Fisher rats were treated with photosensitizer, and a nontoxic intraperitoneal dose of *Clostridium perfringens* epsilon prototoxin (ETXp) followed by light exposure. Post-contrast T<sub>1</sub> MRI scans were used to monitor the degree BBB disruption. F98 tumor cells were implanted into the brains of other animals that were subsequently treated 24 h later with ETXp-PCI BBB opening

followed by the i.p. administration of bleomycin (BLM). PCI delivery of ETXp at low fluence levels demonstrated significant MRI enhancement. No effect on the BBB was observed if photosensitizer and light was given in the absence ETXp. The survival of animals implanted with F98 tumor cells was significantly extended following ETXp-PCI BBB opening and BLM therapy compared to controls. PCI delivered ETXp was effective in opening the BBB in a limited region of the brain. ETXp-PCI mediated BBB opening clearly increased the efficacy of BLM therapy.

**Keywords** Blood brain barrier · Brain tumor · Bleomycin · Photochemical internalization · PDT · *Clostridium perfringens* prototoxin · Targeted opening

### Introduction

Although gross total resection of gliomas, as evaluated on post-operative MRI, is often possible with current available techniques, patients continue to relapse due to the infiltrative nature of these tumors despite post-operative radiation and chemotherapy. Both individual cells and micro-colonies of tumor cells have been shown to infiltrate in or beyond a region of brain-adjacent-to-tumor (BAT)—a zone that may extend several centimeters from the resection margin. This is most probably the reason that, in approximately 80% of all cases, recurrent tumor growth occurs within a 2–3 cm margin of the surgical resection cavity [1]. Infiltrative tumor cells are supplied with nutrients and oxygen by the normal brain vasculature and consequently protected by the BBB: few anti-cancer drugs are capable of crossing this barrier to target these cells [2–4]. For a drug delivery system to be successful at preventing tumor recurrence, transient, and localized targeting of BBB

---

H. Hirschberg (✉) · C.-H. Sun  
Beckman Laser Institute, University of California,  
Irvine, CA, USA  
e-mail: hhirschb@uci.edu

H. Hirschberg · M. J. Zhang · D. Chighvinadze · S. J. Madsen  
Department of Health Physics and Diagnostic Sciences,  
University of Nevada, Las Vegas, NV, USA

H. M. Gach  
Nevada Cancer Institute, Las Vegas, NV, USA

F. A. Uzal  
School of Veterinary Medicine, University of California,  
Davis, San Bernardino, CA, USA

Q. Peng  
Department of Pathology, The Norwegian Radium Hospital,  
Oslo, Norway

disruption in the wall of the resection cavity, following surgical removal of the bulk of the tumor, is necessary.

Attempts to develop pharmaceuticals capable of circumventing the BBB, such as lipid-soluble or water-soluble drugs with high affinities for natural carriers [5–8] have proven only partially successful. Intra-arterial infusion of mannitol, which causes dehydration and shrinkage of endothelial cells, results in opening of the tight junctions and a non-localized BBB disruption. This widespread opening of the BBB results in unwanted side effects since potent cytotoxic drugs gain access to both the tumor as well as normal brain in equal quantities. A number of technical difficulties associated with intra-arterial drug delivery, has prevented the widespread use of this technique [9]. Localized methods of drug delivery that bypass the BBB altogether, such as direct intratumoral injection [10, 11] convection-enhanced delivery [12–14] and controlled release from polymer implants [15, 16] have only shown a modest benefit. Focused ultrasound offers a method to disrupt the BBB noninvasively and reversibly at targeted locations [17, 18]; however, this technique is not well suited to the complex geometry or size of a post-operative resection cavity.

*Clostridium perfringens* epsilon toxin (ETX) is of interest since it is known for its ability to cause widespread but reversible opening of the BBB [19–21]. ETX is synthesized and secreted as a low toxicity precursor prototoxin (ETXp) that is converted to fully active toxin by proteolytic cleavage. Administration of ETXp in a rat model has also been shown to result in a reduction of the endothelium barrier antigen in rat brain endothelial cells accompanied by a reversible opening of the BBB [22].

Photochemical internalization (PCI) is a novel technology that can enhance the delivery of macromolecules in a site-specific manner [23]. The concept is based on the use of specially designed photosensitizers, which localize preferentially in the membranes of endocytic vesicles. Upon light activation, the photosensitizer interacts with ambient oxygen causing vesicular membrane damage resulting in the release of encapsulated macromolecules into the cell cytosol instead of being transported and degraded in the lysosomes. PCI has been shown to potentiate the biological activity of a large variety of macromolecules and other molecules that do not readily penetrate the plasma membrane, including proteins (e.g. protein toxins and immunotoxins), peptides, DNA delivered as a complex with cationic polymers or incorporated in adenovirus or adeno-associated virus, peptide-nucleic acids and chemotherapeutic agents [24–27].

In a previous study, we have demonstrated that 5-aminolevulinic acid (ALA)-mediated PDT was effective in a temporary opening of the BBB in a limited region of the rat brain [28]. Although ALA PDT was effective at opening the BBB, local tissue damage was apparent at fluence

levels just above those required for significant BBB degradation thus limiting the usefulness of this method. In addition, relatively high fluence levels were required for significant BBB disruption.

The purpose of the experiments reported here was to determine the effects of the chemotherapeutic agent BLM on small clusters of tumor cells sequestered in otherwise normal rat brain following localized BBB opening. The orthotopic brain tumor model used in this study consisted of F98 glioma cells in Fischer rats. This model exhibits many of the hallmarks of glioblastoma multiforme (GBM) and, as such, is considered to be highly relevant in therapeutic studies of malignant gliomas [29]. Localized BBB opening was achieved by PCI-mediated delivery of ETXp (termed ETXp-PCI), allowing the passage of BLM in the vicinity of cell implantation. Magnetic resonance imaging was used to determine the concentration and volume of gadolinium (Gd) contrast enhancement to infer the extent of BBB disruption and to track BBB disruption dynamics.

## Materials and methods

### Experimental animals

Inbred male Fischer rats (Simonsen Laboratories, Inc, Gilroy, CA) weighing about 350 g were used in this study. Animal care and protocols were in accordance with institutional guidelines. Animal holding rooms were maintained at constant temperature and humidity on a 12 h light and dark schedule at an air exchange rate of 18 changes per hour. For the surgical procedures, animals were anaesthetized with Pentobarbital (25 mg kg<sup>-1</sup> i.p.). Buprenorphin (0.08 mg kg<sup>-1</sup> s.c.) as a post-operative analgesic was administered to animals following surgery and twice per day for 3 days thereafter. All animals were euthanized at the end of the study, or at the first signs of distress. Euthanasia was accomplished with an overdose of Pentobarbital (100 mg kg<sup>-1</sup> i.p.).

### Cell lines

The F98 glioma cell line was originally derived from transformed fetal CD Fischer rat brain cells following exposure to ethyl-nitrosourea on the 20th day of gestation [29]. The F98 cells were grown as monolayers in DMEM medium (Invitrogen Corp., Carlsbad, CA) with 10% fetal bovine serum (FBS), 25 mM HEPES buffer (pH 7.4), penicillin (100 U ml<sup>-1</sup>) and streptomycin (100 µg ml<sup>-1</sup>) at 37°C and 5% CO<sub>2</sub>. To generate multicell tumor spheroids, cells (70% confluence) were harvested with trypsin and resuspended in DMEM to a final volume of 5 ml. The cell suspension was transferred to a petri dish coated with a 1:1

solution of 2% agar and  $2\times$  DMEM and fresh medium were added to a total volume of 20 ml. The dish was placed in an incubator and cell clusters were observed within 24 h. After a week, spheroids were transferred to a non-coated dish for culturing. Approximately 24 h prior to experimentation, a microscope was used to manually select spheroids of approximately 450  $\mu\text{m}$  diameter.

#### Direct BLM or ETXp toxicity assay

Purified ETXp was obtained from the School of Veterinary Medicine, University of California, Davis, San Bernardino, Ca. ETXp was prepared from an overnight culture of *C. perfringens* type D (strain NCTC 8346) in tripticase–yeast–glucose medium, under anaerobic conditions at 37°C. The overnight cultures were centrifuged at 10,000 rpm for 30 min at 4°C and the supernatant containing epsilon toxin was saved for toxin purification. The toxin was then precipitated by ammonium sulphate. Two columns were prepared with DEAE and CM Sepharose (Pharmacia, Sweden), respectively, equilibrated in 10 mM Tris, pH 7.5. The toxin was applied to the DEAE column and the effluent was monitored at 220 nm. The initially eluted peak was saved and applied to the CM column. Again the effluent was monitored at 220 nm and the first peak was collected, dialyzed against distilled water and freeze-dried. This product was shown to contain pure epsilon prototoxin when tested by SDS PAGE. Prior to its use in these experiments, the prototoxin was reconstituted in Ringer and activated by incubation at 37°C during 30 min with 0.1% trypsin (Sigma).

F98 cell monolayers were incubated in increasing concentrations (0.1–10  $\mu\text{g ml}^{-1}$ ) of BLM-containing medium (Sigma, St. Louis, MO) or increasing concentrations of ETXp (1:200–1:25 dilution) for 4 h. Following exposure to BLM or ETXp, the cell monolayers were washed, harvested with trypsin, counted using a Coulter Counter (Beckman Coulter, Model Z, Fullerton, CA) and then incubated at various cell densities in complete media for 11–14 days to allow for colony growth. Colonies that grew from the surviving cells were stained with crystal violet and counted (>50 cells/colony).

#### ETXp-PCI toxicity assay

F98 cell monolayers were incubated in serum-containing medium with 1  $\mu\text{g ml}^{-1}$  photosensitizer (aluminum phthalocyanine disulfonate; AIPcS<sub>2a</sub>) for 18 h, washed 3 times with medium and incubated in BLM (0.25  $\mu\text{g ml}^{-1}$ ) or *Cl. p* (dilution 1:50) containing medium for 4 h. Following incubation, monolayers were washed once with medium, resuspended in drug-free medium, and irradiated with 670 nm light from a diode laser (Intense Ltd, North

Brunswick, NJ). The cells were exposed to a radiant exposure of 1.5 J  $\text{cm}^{-2}$  delivered at a light irradiance of 5 mW  $\text{cm}^{-2}$ . PDT-only controls received AIPcS<sub>2a</sub> and light as described above but no drug was administered. BLM or ETXp controls received no photosensitizer or light. Following irradiation, cells were harvested and prepared for colony growth as described in the previous section. A total of three experiments were performed.

#### Migration assay

The cell migration assay has been described previously [30]. Briefly, the matrix used in these experiments consisted of a collagen gel composed of 70% type I rat tail collagen at a concentration of 4 mg  $\text{ml}^{-1}$ , 20%  $5\times$  DMEM and 10% reconstituted buffer made of 260 mM sodium bicarbonate and 200 mM HEPES. Single F98 tumor spheroids (450  $\mu\text{m}$  diameter) were placed in imaging dishes coated with a thin layer of dried rat tail type I collagen. After an hour to allow for spheroid adhesion, 200  $\mu\text{l}$  of the collagen gel matrix was deposited over the spheroid and allowed to gel. The cultures were then overlaid with 400  $\mu\text{l}$  of culture medium containing 10% FBS and BLM (0.1–1  $\mu\text{g ml}^{-1}$  Sigma, St. Louis, MO) for 4 h, washed once with medium and resuspended in drug-free medium. Within a few hours of spheroid placement in the collagen type I gel, individual cells began to detach from the surface of the spheroid and migrate into the surrounding matrix. Eighteen hours following implantation, the cells had migrated to an average distance of 2–300  $\mu\text{m}$ . Invasion distance was calculated daily as the distance in micrometers from the spheroid edge to the population of cells most distant from the spheroid edge.

#### ETXp-PCI induced BBB degradation in non-tumor-bearing rats

Non-tumor-bearing animals were divided into three groups: (1) PDT controls, (2) ETXp controls, or (3) PCI (PDT + ETXp). Animals in the ETXp-only group were administered 0.7 ml (i.p.) of 1:10, 1:50 or 1:100 dilutions of ETXp stock solution (1 mg  $\text{ml}^{-1}$ ). The toxicity and extent of BBB disruption induced by different concentrations ETXp were evaluated from animal survival and MR images.

Animals in the PCI treatment group were injected with AIPcS<sub>2a</sub> (1 mg  $\text{kg}^{-1}$  i.p.) and 48 h later, a 1:100 dilution of ETXp was administered i.p. At the time of light treatment, anaesthetized rats were fixed in a stereotactic frame (David Kopf Instruments, Tujunga, CA), a skin incision was made exposing the skull and an optical fiber coupled to a 670 nm diode laser was placed in contact with the surface of the skull 1 mm posterior to the

bregma and 2 mm to the right of the midline. Surface light irradiation was given approximately 60 min after ETXp administration at light fluences of 0.5, 1.0 and 2.5 J at a fluence rate of 10 mW. Following treatment, the wound was closed with sutures and the rats removed from the frame. PDT controls consisted of photosensitizer and light treatment as described above but in the absence of ETXp administration.

#### BLM treatment of tumor cell injected animals

The protocol for these experiments was as follows. Newly implanted glioma cells were used as a proxy for infiltrating cells remaining in the resection margin following surgical removal of bulk tumor. BBB opening was initiated 24 h following cell inoculation—a time considered to be insufficient to allow for the development of bulk tumor and BBB degradation, but long enough for the cells to form small sequestered micro-clusters protected by an intact BBB. To establish intracranial tumors, anaesthetized rats were fixed in the stereotactic frame as previously described. The skin was incised and a 1.0-mm burr hole was made at the following coordinates: 1 mm posterior to the bregma, 2 mm to the right of the midline and at a depth of 2 mm. The injection device consisted of a 30-G blunt cannula connected through a catheter (Hamilton Co., Reno, NV) to an infusion pump (Harvard Apparatus, Holliston, MA). The cannula was fixed in the electrode holder of the stereotactic frame, and then vertically introduced into the brain. A total of 10,000 cells in 5  $\mu$ l PBS were injected into the brain during a period of 2 min. Following injection, the cannula was kept in place for 2 min, and slowly retracted to prevent the spread of tumor cells. Closure was done with bone wax and sutures. Twenty-four hours later, ETXp was administered intraperitoneal at a concentration described previously. At the time of light treatment, anaesthetized rats were fixed in the stereotactic frame the skin incision was reopened exposing the skull and an optical fiber was placed in contact with the surface of the skull at the point of cell implantation. Surface light irradiation was given approximately 60 min after ETXp administration at a light fluence levels of 1.0 J at a fluence rate of 10 mW. Following treatment the wound was closed with sutures and the rats freed from the frame. Bleomycin (4 mg/kg) was injected i.p. at the time of light treatment and repeated five additional times at 12 h intervals. Control animals received no treatment or PDT and BLM in the absence of ETXp.

#### MR imaging

Isoflurane-anesthetized animals were imaged on days 1, 3, 5, 8 and 18 post-PCI treatment in a 7.0 T animal MR

scanner (Bruker Corp., Billerica, MA). A small surface coil was placed on top of the target area and 0.8 ml of a Gd-based contrast agent (Multihance: Bracco Diagnostics, Inc, Princeton, NJ), was injected i.p.  $T_1$ -weighted (TR = 700 ms; TE = 14 ms) post-contrast MR image were taken 15–20 min after contrast injection. Since Multihance, with a molecular weight of 1058.2, is too large to cross the intact BBB, any contrast enhancement evident on  $T_1$ -weighted images was taken as direct evidence of BBB disruption induced by the corresponding treatment. To evaluate the extent of edema reaction,  $T_2$ -weighted images (TR = 4,200 ms; TE = 36 ms) were also acquired for each animal. Gd concentration was estimated as follows. Four calibration tubes with known Gd concentrations in gray-matter-mimicking saline were scanned and the intensities analyzed using MIPAV (Medical Image Processing, Analysis & Visualization) software. It was assumed that the relationship between the Gd concentration and the signal intensities in white and gray matter were similar to that of the calibration tubes and therefore, the calibration curve derived from these measurements could be extrapolated to brain tissue as previously described [28].

#### Data analysis

The extent of BBB disruption for each treatment was evaluated from the degree of contrast enhancement observed on  $T_1$  post-contrast images. The qualitative analyses of contrast and edema volumes were performed using MIPAV software. Both contrast and edema volumes were first manually contoured on each  $T_1$  slice. The total volume was then calculated automatically by the software according to the following equation:  $V = \sum_i (S_i * T)$  cm<sup>3</sup> where  $S_i$  represents the contrast area contoured on each slice and  $T$  represents the image slice thickness. A thickness of 1.0 mm was used in all MR images acquired in this study.

#### Histological preparation

Animals were sacrificed 21 days following ETXp-PCI BBB opening and their brains extracted. The brains were sectioned at the point of light application and fixed by immersion in 10% buffered (pH 7.2) formalin prior to paraffin embedding. Four micrometer thick coronal sections were obtained from the original cut surface representing the position of the light applicator. The sections were routinely processed for the production of hematoxylin and eosin (H&E) sections and examined under a light microscope by an independent pathologist blinded to the treatment modes.

**Results**

**In vitro studies**

The direct cytotoxic effects of either BLM or ETXp on F98 monolayers are shown in Fig. 1a and b. The cells were exposed to either agent for 4 h and then assayed with respect to their ability to form new cell colonies after 11–14 days in culture. Increasing concentrations of BLM caused a decreasing survival of colony forming cells and at a concentration of 5  $\mu\text{g ml}^{-1}$  less than 5% of the cells survived (Fig. 1a). In contrast, ETXp did not appear to be toxic to the monolayers, even at the highest concentration tested (Fig. 1b).

In order to determine the effects of ETXp-PCI in vitro, experiments were performed on F98 cell monolayers. The monolayers were incubated with the photosensitizer for 18 h, followed by 4 h incubation with ETXp (dilution 1:50) and thereafter irradiated with 670 nm light ( $1.5 \text{ J cm}^{-2}$ ). PDT-only controls received AlPcS<sub>2a</sub> and

light but no ETXp. ETXp controls received neither photosensitizer nor light. As can be seen in Fig. 2a, there was no significant increase in the toxic effects of PCI-mediated delivery of ETXp compared to the PDT controls. In contrast, BLM-PCI produced significant cell toxicity compared to both PDT and BLM control cultures (Fig. 2b). Only 24% of the ETXp-PCI BLM treated cultures survived treatment compared to 78% and 74% for the PDT and BLM control cultures respectively. The BLM-PCI effect was significantly higher than the additive effects of PDT and BLM on these cells.

Both tumor cell proliferation and migration are important for tumor progression in the brain. The ability of BLM to inhibit F98 cell migration into a collagen matrix in vitro is shown in Fig. 3. High concentrations of BLM that clearly inhibited the ability of cells to form colonies had minimal effect on cell mobility (Fig. 3). Even at a BLM concentration of 1  $\mu\text{g ml}^{-1}$ , which produced a 65% inhibition of F98 cell proliferation, only a slight decrease in cell migration was observed.

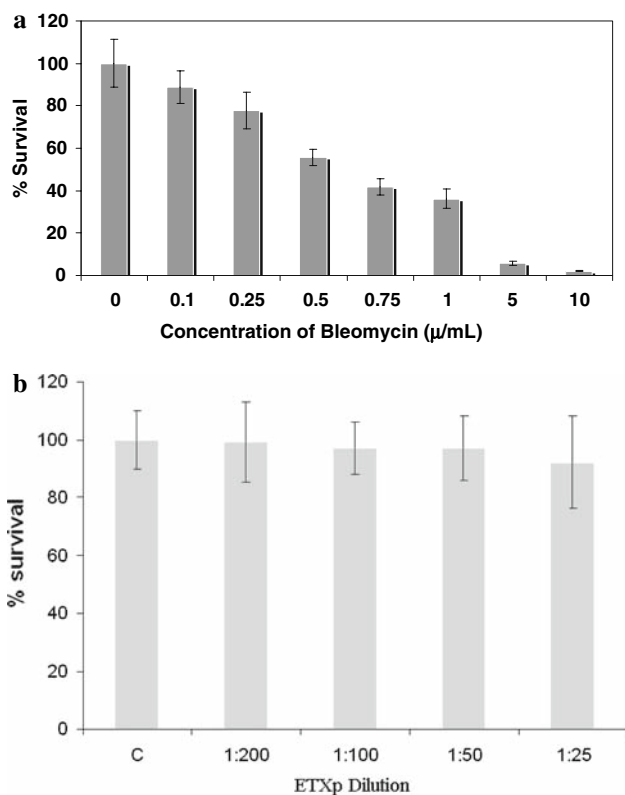


**Fig. 1** Cytotoxic effects of BLM or ETXp on F98 monolayers. F98 cell monolayers were incubated in increasing concentrations. **a** (0.1–10  $\mu\text{g ml}^{-1}$ ) of bleomycin-containing medium or increasing concentrations of **(b)**: ETXp (1:200–1:25 dilution). BLM had a significant inhibitory effect on the ability of the cells to form colonies while ETXp had little effect. Data points represent the mean of 3 experiments  $\pm$  standard error

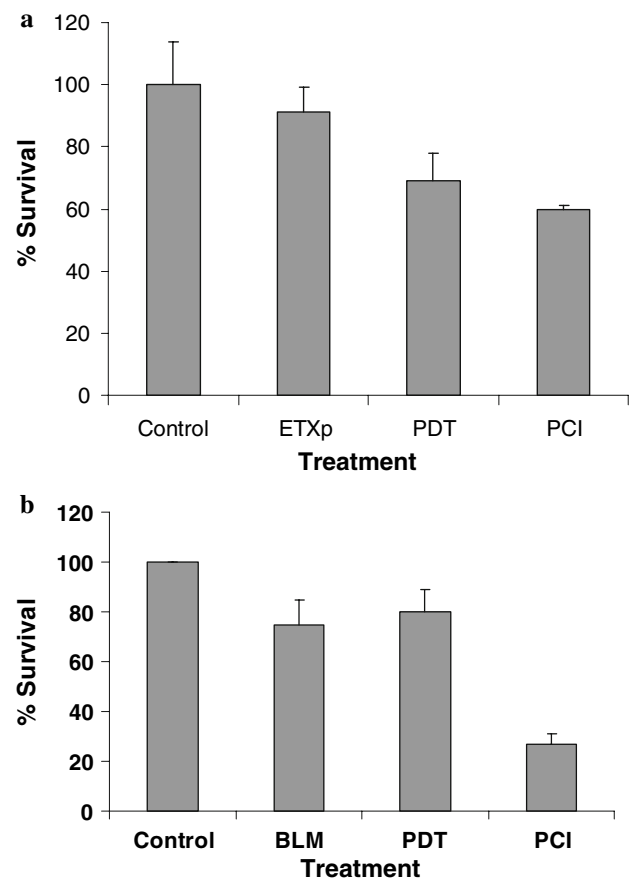


**Fig. 2** Effects of ETXp-PCI or BLM-PCI on F98 monolayers. **a** ETXp-PCI had no significant toxic effect on F98 cells in contrast to **(b)**: the effect of BLM-PCI. Control groups consisted of; no treatment, ETXp, or BLM no light, and PDT only. Data points represent the mean of 3 experiments  $\pm$  standard error

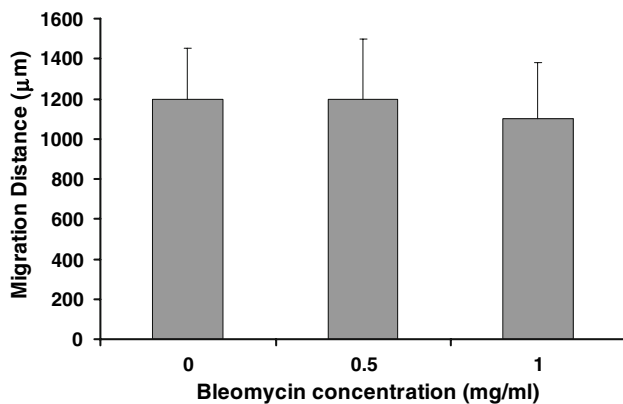


**Fig. 3** Effects of BLM on F98 cell migration from multicell spheroids. Single F98 tumor spheroids were implanted in a collagen matrix overlaid with culture medium containing bleomycin ( $0.1\text{--}1\ \mu\text{g ml}^{-1}$ ). Invasive distance was calculated after 4 days in culture as the distance in  $\mu\text{m}$  from the spheroid edge to the most distant population of invasive cells. BLM had little effect on cell migration. Each data point represents the mean ( $\pm$ standard error) of three experiments

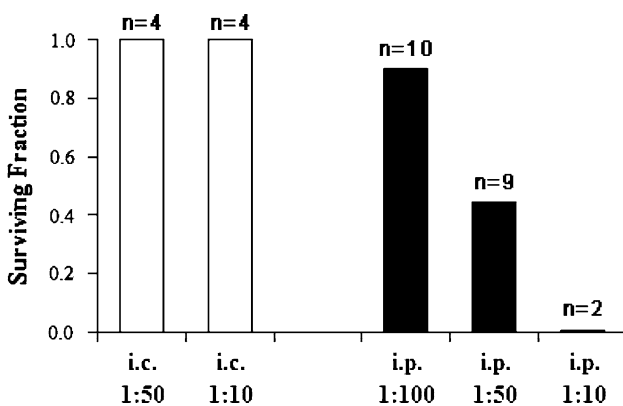


**Fig. 4** Surviving fraction of animals subjected to ETXp. Two administration routes were compared: direct intracranial injection (i.c.;  $5\ \mu\text{l}$  total volume), and intraperitoneal injection (i.p.;  $0.7\ \text{ml}$  total volume). The  $n$  value above each data bar indicates the total number of animals used per group

#### In vivo ETXp toxicity

The toxicity of ETXp delivered either by intra peritoneal (i.p.) or intracranial (i.c.) injection was evaluated in a number of animals. Animals surviving for more than 20 days were considered to have survived. As shown in Fig. 4, all animals receiving ETXp i.c. survived. In contrast, the delivery of ETXp to animals via i.p. injection proved to be much more toxic resulting in death of all animals receiving a dose of 1:10. It is interesting to note that, although i.p. administration resulted in significant mortality, no evidence of localized contrast (BBB disruption) was observed on MR images in animals that survived (data not shown). Overall, the results suggest that i.c.

injection or i.p. injection of ETXp at a dilution of 1:100 or higher were well tolerated and therefore provided the rationale for its use in the BBB experiments.

#### PDT and PCI-induced BBB disruption

Localized regions of increased signal intensity on  $T_1$ -weighted MRI scans were used as a marker for BBB disruption in the rat brain. Both the volume of the enhancing region and the signal intensity were measured at specific time intervals following i.p. contrast injection. Forty-eight hours following AlPcS<sub>2a</sub> injection ( $1\ \text{mg kg}^{-1}$  i.p.) light treatment was given to three groups of rats ( $n = 4$  per group) to a fluence level of 0.5, 1.0 or 2.5 J using a fluence rate of 10 mW. Typical post-contrast MRI scans performed 3 days after PDT (photosensitizer + light) or PCI (ETXp, photosensitizer + light), are illustrated in Fig. 5. The scans were taken 15 min following i.p. contrast injection. Clear evidence of significantly increased local BBB disruption is seen following light treatment in the presence of ETXp compared to PDT treatment for the two lowest fluence levels. This is evidenced by the localized contrast enhancement observed directly below the position on the skull where the light delivery fiber tip was positioned. Average contrast volumes and intensities for the four animals in each group are shown in Fig. 6a and b respectively. The degree of contrast enhancement (and hence BBB disruption) is clearly fluence dependent for both PDT and PCI. Zero to minimal enhancement was observed for PDT at the two lowest fluences (0.5 and 1 J) investigated. In contrast, significant enhancement was seen in the ETXp-PCI animals. At a fluence of 2.5 J, the PDT effect was so pronounced that the addition of ETXp had no apparent effect on BBB disruption. The concentration of the contrast medium in the brain (calculated from the calibration curve derived from the Gd standard tubes shown in Fig. 7a and b) is shown in Fig. 8. Contrast concentrations of 0.2 and  $1.4\ \text{mg ml}^{-1}$  for PDT and PCI treatment respectively were obtained for a 1 J fluence level. In the absence of photosensitizer (light-only control), high fluences (2.5 J) demonstrated no apparent increased signal in the region of light treatment compared to normal brain.

#### Histological analysis

Coronal H&E sections (a and c) obtained from rat brains 21 days post treatment and corresponding  $T_1$  MRI scans acquired 3 days post-treatment (b and d) are shown in Fig. 9.

In tissue volumes subjected to ETXp-PCI and light no significant histological changes were observed in coronal sections obtained from animals exposed to fluences of 0.5 J (data not shown) or 1 J (Fig. 9a). At fluence levels above 2.5 J, even in the absence of ETXp a focally extensive area

**Fig. 5** T<sub>1</sub>-weighted MRI contrast enhanced images showing focal contrast enhancement directly below the light source. Forty-eight hours following ALPcS<sub>2a</sub> injection (1 mg kg<sup>-1</sup> i.p.) light treatment was given to three groups of rats (*n* = 4 per group) to a fluence level of 0.5, 1.0 or 2.5 J using a fluence rate of 10 mW. The scans were performed 3 days after PDT (photosensitizer + light) or PCI (ETXp, photosensitizer + light). The scans were taken 15 min following i.p. contrast injection

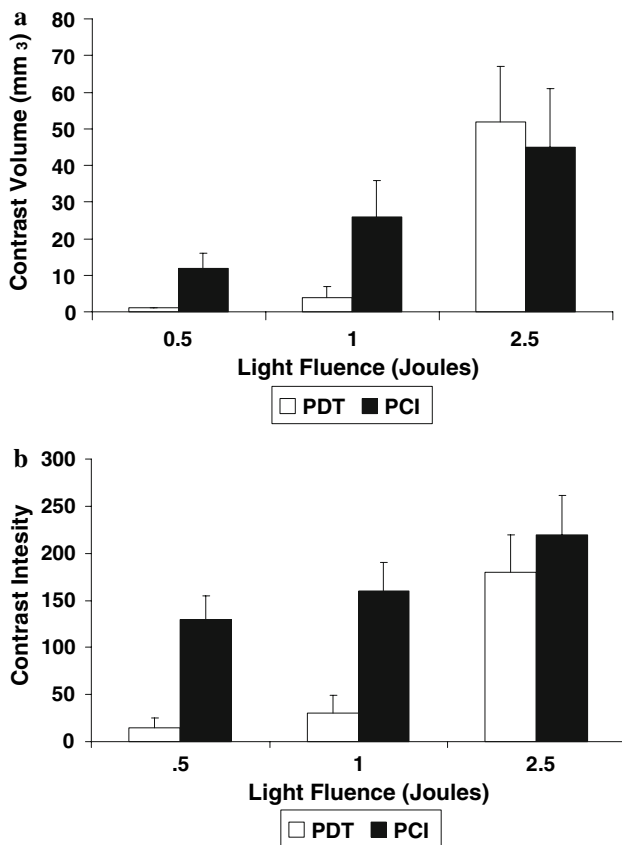
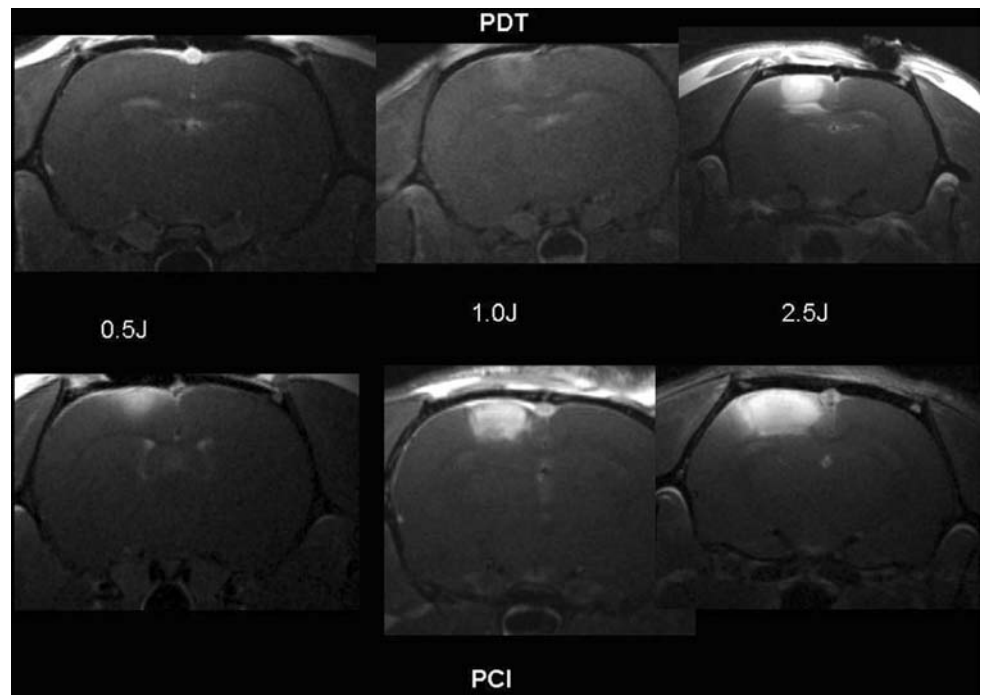


**Fig. 6** **a** Average contrast volume and **b** signal intensity measured from MRI scans performed 3 days post PDT or ETXp-PCI treatment for three light fluences (0.5, 1, 2.5 J; fluence rate = 10 mW). Each data point represents the mean ( $\pm$ standard error) of four animals

of necrosis and degeneration of brain parenchyma and infiltration of lymphocytes, plasma cells and foamy macrophages (Gitter cells), was apparent in the area directly below the application of light (Fig. 9c). Some of the Gitter cells contained hemosiderin which is suggestive of hemorrhage. Blood vessels in these sections showed hypertrophic and hyperplastic endothelium.

Time course of BBB disruption

Of particular interest is the time duration and evolution of the ETXp-PCI BBB disruption since this represents the therapeutic window for drug delivery. Typical post-contrast MRI scans performed 1, 3, 5, and 18 days after ETXp-PCI treatment are illustrated in Fig. 10a–d respectively. ETXp was given i.p. at a dilution of 1:100 and a light fluence of 1 J was employed. The scans were taken 15 min following i.p. contrast injection. Enhancement volumes peaked on day 3 suggesting maximum BBB disruption at that time. Thereafter, contrast volumes were observed to decrease and by day 11, only trace amounts of contrast were observed in the 0.5 and 1 J animals. Animals treated with 2.5 J demonstrated significant contrast volumes even at 14 days post-treatment. Figure 11 shows the average BBB opening time as inferred from enhancing volumes for four ETXp-PCI and four PDT control animals. The optimum therapeutic drug delivery window appeared to be between days 2 and 5 following BBB opening.

In order to study the dynamics of flow into the region of the brain where the BBB was opened by ETXp-PCI, 4

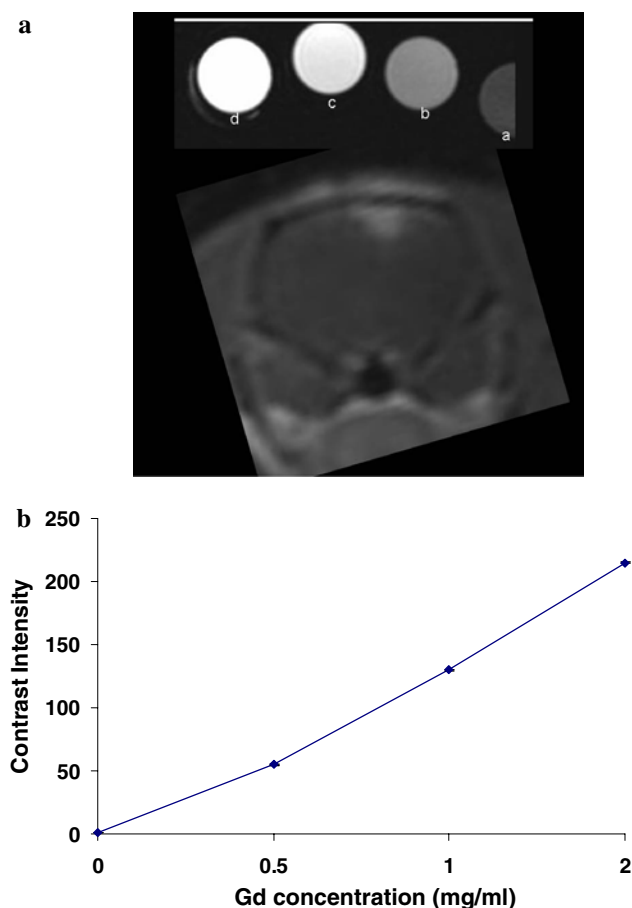


**Fig. 7** **a** T1-weighted MR images of a ETXp-PCI treated rat along with four calibration tubes with Gd concentrations of 0 (*a*), 0.5 (*b*), 1 (*c*) and 2 (*d*) mg/ml. **b** MRI signal intensity as a function of Gd concentration derived from the reference tubes shown. The value of the intensity in tube *a* (saline) has been subtracted in all cases

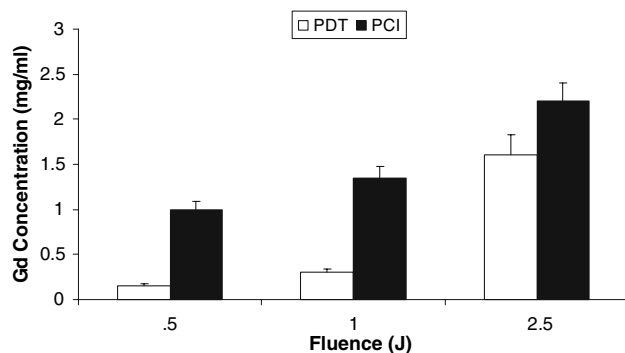


**Fig. 8** Average contrast concentrations as a function of fluence level. The concentrations were derived from MRI scans performed 3 days post PDT or ETXp-PCI treatment for three light fluences (0.5, 1, 2.5 J; fluence rate = 10 mW). Each data point represents the mean ( $\pm$ standard error) of four animals

animals were scanned 5 and 60 min following i.p. contrast injection. Disruption of the BBB results in flow of blood plasma components into the surrounding brain tissue

causing edema formation. This is clearly evident in the  $T_2$ -weighted scan shown in Fig. 12a. The region of edema was localized to the illuminated portion of the brain in all of the treated animals. As can be seen from the  $T_1$  MRI scan taken 5 min post i.p. contrast injection (Fig. 12b) enhancement appears mainly around the periphery of the edema region. The animal was rescanned 60 min after contrast injection and now the contrast was evenly distributed throughout the volume of illuminated brain tissue (Fig. 12c).

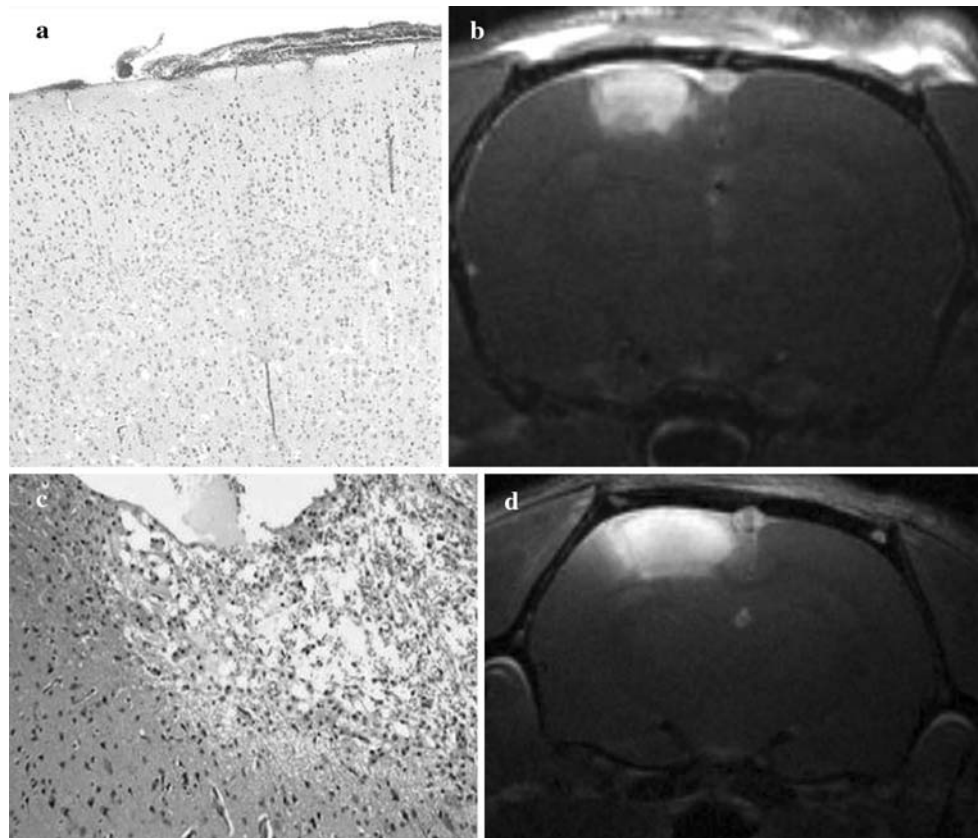
#### Effects of BLM on tumor formation

Fifteen animals were divided into three groups: non-treated controls (group 1), PDT-BLM controls (group 2) and ETXp-PCI-BLM (group 3). Animals in groups 2 and 3 were injected with  $AlPcS_{2a}$  ( $1 \text{ mg kg}^{-1}$ , i.p.) and 24 h later  $1 \times 10^4$  cells were implanted. After an additional 24 h, animals in group 3 were given ETXp i.p. and 1 J of light was delivered to both groups 2 and 3. BLM ( $4 \text{ mg kg}^{-1}$ ) was injected i.p. at the time of light treatment and thereafter, every 12 h over 3 days for a total of six doses ( $24 \text{ mg kg}^{-1}$ ). Animals were euthanized at the first signs of distress due to increased intracranial pressure, neurological deterioration or weight loss of more than 10%. Kaplan–Meier survival curves are shown in Fig. 13. Tumor cell injection was lethal in 100% of controls with no survivors past day 33. The animals in the BLM-PDT group all succumbed but their survival was significantly increased compared to controls ( $P < 0.01$ ). In contrast, 60% of the animals in the ETXp PCI-BLM group survived more than 70 days and one animal was considered a long-term survivor.

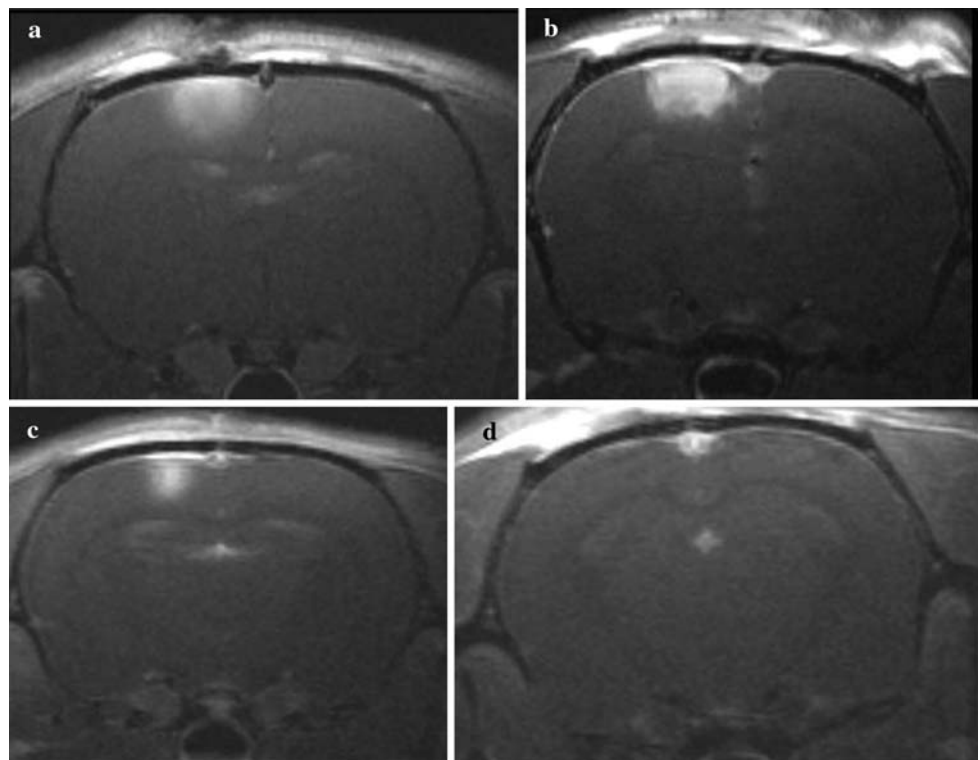
#### Discussion

The inherent tendency of glial tumors to infiltrate normal brain tissue significantly limits the effectiveness of conventional treatments. Although surgical resection reduces the pressure effects of the bulk tumor, it is the diffusely invading tumor cells beyond the resection margin that are responsible for the damage to normal brain parenchyma which ultimately results in the death of the patient. In this study, we have employed the anti-neoplastic agent bleomycin, a glycopeptide antibiotic which acts by induction of DNA strand breaks, applied through a targeted opening of the BBB to inhibit tumor formation in the rat brain. Newly implanted tumor cells were used to mimic the characteristics of infiltrating cells remaining in the resection margin usually found following surgical removal of bulk tumor. Localized BBB opening was performed 24 h after cell inoculation. This is an insufficient time to allow for the

**Fig. 9** Effects of fluence level on tissue disruption. Coronal H&E sections (**a**, **c**) from rat brains corresponding to T1 contrast MRI scans (**b**) and (**d**). The sections were taken 21 days post-treatment and the T<sub>1</sub>-weighted post-contrast images were acquired 3 days post-treatment. In the area exposed to the highest fluence level (close to the dura) no significant pathology (**a**) was observed following delivery of 1 J. At a fluence level of 2.5 J, extensive infiltration of lymphocytes and macrophages, some loaded with hemosiderin, was apparent



**Fig. 10** T<sub>1</sub>-weighted MRI contrast enhanced images showing focal contrast enhancement at: **a**—1, **b**—3, **c**—5 and **d**—18 days post-treatment. ETXp-PCI treatments using 1 J were performed at a fluence rate of 10 mW. All animals were scanned 15 min following i.p. contrast injection. A localized contrast enhancement is clearly seen 1–5 days following light treatment



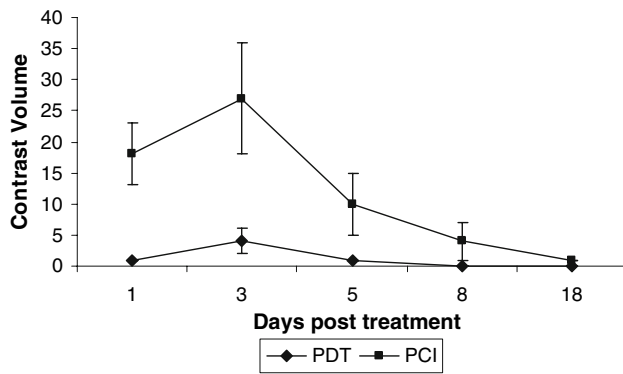


**Fig. 11** Average time course of BBB opening induced by PDT or ETXp-PCI. The animals ( $n = 4$  per group) received  $1 \text{ mg kg}^{-1}$  AIPcS<sub>2a</sub> and a light fluence of 1 J. The PCI group of animals also received an i.p. injection of ETXp at a concentration of 1:100. Both PDT and PCI animals were scanned on days 1, 3, 5, 8 and 18 after treatment. All T<sub>1</sub> post-contrast images were taken 15 min following i.p. contrast injection

development of bulk tumor and BBB degradation, but long enough for the cells (doubling time of approximately 18 h) to form small sequestered micro-clusters which are protected by an intact BBB.

The data presented in Fig. 1 show that while BLM had a pronounced effect on the proliferation of F98 cells in vitro, ETXp did not. This is in agreement with studies suggesting that ETX-induced effects occur specifically in cells expressing the tight junction proteins claudin-3 and/or claudin-4, which function as low- and high-affinity receptors for ETX, respectively [31, 32]. Other recent studies show little or no claudin-3 or claudin-4 mRNA expression in whole-brain tissue, consistent with the fact that these proteins are expressed usually in cells of epithelial origin such as endothelial cells, whereas glia cells and neurons are of mesenchymal origin [33]. The data illustrated in Fig. 2a show that there is no significant difference in survival of cells exposed to ETXp-PCI and PDT, suggesting that the observed cytotoxicity in both groups was due entirely to

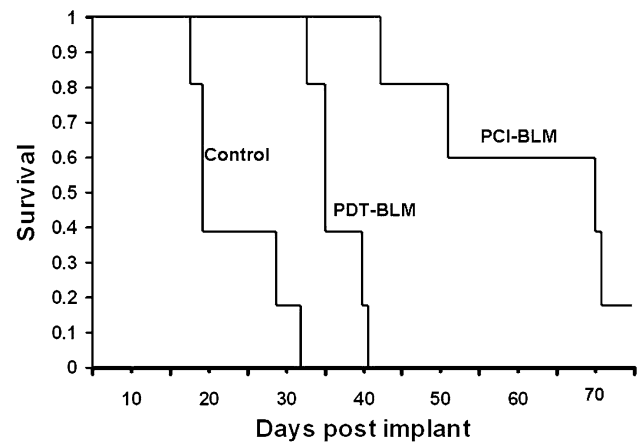


**Fig. 13** Kaplan–Meier survival of tumor cell implanted animals. All animals received  $1 \times 10^4$  cells i.c. Three groups were followed: non-treated controls, PDT-BLM controls (AIPcS<sub>2a</sub> + 1 J), ETXp-PCI BLM experimental group (AIPcS<sub>2a</sub> + ETXp + 1 J); BLM ( $4 \text{ mg kg}^{-1}$ ) was injected i.p. twice daily for 3 days

the PDT effect. ETXp proved however to be highly toxic in animals when given i.p. in high concentrations (Fig. 4). A plausible explanation for the observed toxicity is protease-induced prototoxin activation in the body. This could occur following internalization in rat peritoneal macrophages and subsequent conversion to toxin via lysosomal degradation. Absorption of the activated toxin via the peritoneum may have produced the toxic effects observed following administration of high concentrations ETXp. Since glia derived F98 cells most probably lack the receptors (claudins) for the prototoxin, it will not be internalized and therefore not converted to the active toxin in these cells. In contrast, brain capillary endothelial cells are rich in both claudin-3 and -4 since these cells form tight junctions, and therefore can convert the prototoxin into the active toxin. Binding of the epsilon toxin to the brain capillary endothelium results in a reversible loss of BBB integrity and hence increased vascular permeability. For example, in studies using horse-radish peroxidase as a tracer, it has

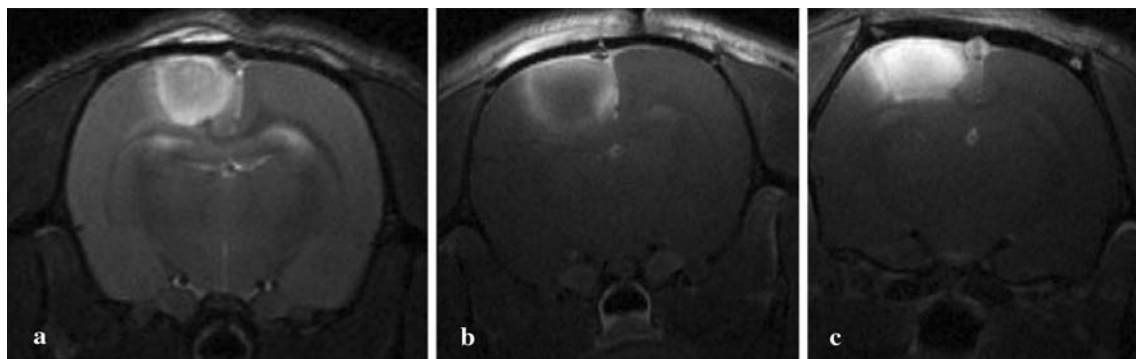


**Fig. 12** Dynamics of local contrast flow. **a** T<sub>2</sub>-weighted scan showing edema localized to the illuminated portion of the brain. **b** T<sub>1</sub> MRI scans taken 5 min and **c** 60 min post i.p. contrast injection

been shown that this enzyme leaks from murine brain blood vessels within 1 h of intravenous toxin administration [34].

It is hypothesized that the biological effects of the ETXp on the BBB is potentiated by PCI, but only in areas of the brain exposed to adequate light fluences. Due to this potentiation effect, sub-threshold ETXp doses will be sufficient to open the BBB, but this low ETXp dose will be inadequate to open the BBB in regions where the light fluence is insufficient to evoke the PCI effect. The validity of this hypothesis is supported by the results presented in Figs. 5 and 6 which show that increasing light fluences (0.5–2.5 J) resulted in increasing BBB disruption. In a related study, we have shown that ALA-mediated PDT at relatively high fluences (9–26 J) could also produce BBB degradation [28]. In this case, the BBB opened after 2 h but was essentially closed 72 h later. In contrast, the time course for ETXp-PCI BBB opening was much longer (Figs. 10 and 11) peaking at day three or four and closing by day 14. This is clinically relevant as it would provide an effective long interval for drug delivery. As evidenced from histological sections (Fig. 9a), the effects of ETXp-PCI were reversible only if the fluence level was kept at or below 1 J since no permanent damage was observed at these fluence levels. In contrast, higher fluence levels, where the direct PDT effect on endothelial cells predominated, resulted in significant localized tissue damage (Fig. 9c). Based on histological evaluation, the tissue damage and immune cell infiltration observed in regions close to the light source were consistent with cerebral ischemia resulting in a localized stroke. This is consistent with the intense contrast enhancement observed on MR images: contrast enhancement is considered to be one of the signatures of BBB breakdown in cerebral ischemia.

Although a detailed understanding of the reversible low light fluence BBB disruption seen in these experiments is at present unknown, a direct effect on the capillary endothelial cells is the most probable cause. This would include direct interaction of ETX on the endothelial cell cytoskeleton in the illuminated regions that could lead to cell rounding and contraction, with the formation and/or enlargement of endothelial gaps that have previously been described in response to PDT [35]. Additionally, low fluence rate/low fluence PDT has been demonstrated to enhance the delivery of macromolecular drug carriers, in particular liposomally encapsulated doxorubicin, into murine colon carcinoma tumors growing in the shoulders of mice [36].

In this study, newly implanted F98 cells were used to mimic the characteristics of infiltrating cells. F98 glioma growth in vitro and in vivo morphology have been described in detail, and the tumor has been classified as an anaplastic or undifferentiated glioma with many characteristics that

closely resemble those of human GBM and anaplastic astrocytoma. As few as 100 tumor cells injected into the brains of Fischer rats have been shown to be lethal [29]. This tumor has also been shown to be refractory to several forms of chemotherapy and radiotherapy in vivo and, as such, is considered a good model for evaluating experimental therapies where survival is the endpoint [37]. In the survival experiments shown in Fig. 13, 10,000 cells were inoculated. Therefore, a cell kill of 99% would be required in order to completely prevent tumor formation. Only one animal seemed to be “cured” but the survival time in the ETXp-PCI group was significantly increased compared to non-treated controls or controls that received PDT-BLM. Since BLM did not appear to inhibit F98 cell migration (Fig. 3) it is conceivable that some cells were able to migrate into an area of the brain where the BBB was still intact: i.e. out of the region where the fluence level was sufficient to open the BBB. These cells could potentially give rise to delayed tumor formation since migratory cells have a lower proliferation rate and are more resistant to apoptosis [38]. The in vitro data shown in Fig. 1a suggest, that a BLM concentration in excess of  $5 \mu\text{g ml}^{-1}$  would be required to eliminate more than 90% of the F98 cells. In the MR imaging studies, average contrast concentrations in the treatment volumes (1 J light fluence) were 1.4 and  $0.2 \text{ mg ml}^{-1}$  in ETXp-PCI and PDT groups, respectively (Fig. 8). Since 375 mg of Gd contrast was given i.p. to each animal prior to scanning, the concentration in the region of BBB opening would represent less than 0.5% of the injected dose. If this ratio of total dose to brain concentration is similar for BLM, this suggests a drug concentration of approximately  $7.5 \mu\text{g ml}^{-1}$  was obtained in the vicinity of the implanted cells following i.p. administration of 1.5 mg BLM. According to the in vitro results, this concentration is likely inadequate for the elimination of 99% of the implanted cells. Based on these calculations, it is not surprising that most of the animals developed tumors. Even so, the treatment resulted in extended survival compared to controls. It should be pointed out that since BLM has a higher molecular weight than Gd contrast, the actual concentration of the drug in the vicinity of the implanted cells was likely overestimated. Since increased survival was the endpoint for BLM efficacy, no attempt was made to measure the actual BLM concentration in the brain.

Increased localized tissue pressure due to edema formation following localized BBB disruption is a potential problem in a compressed brain, such as the rat model used in this study. As shown in Fig. 12, the increased intracranial pressure due to tumor compression caused a significant reduction in contrast flow rate. From a clinical point of view, this effect can be managed effectively post-operatively in patients that have undergone decompressive cytoreductive surgery. In this case, light could be applied via

an indwelling balloon applicator implanted in the resection cavity and the BBB disruption would be limited to the walls of the cavity [39].

ETX has recently been shown to cause rapid destruction of certain types of cancer cells expressing the ETX receptors claudin-3 and claudin-4. Unfortunately, the utility of this toxin is limited by systemic toxicity because its receptors are expressed in numerous organs as evidenced from the data presented in Fig. 4. The results of the present study suggest however that, under the appropriate conditions, PCI is a safe and efficient method for the selective disruption of the BBB in rats. Due to ETX or ETXp toxicity, it is highly unlikely that ETXp-based PCI approaches will be used in human clinical protocols. Nevertheless, the results presented herein provide the basis for further PCI studies using non-toxic vasoactive compounds including bradykinin and its analogs, leukotrienes and histamine [40–42].

**Acknowledgments** The authors are grateful for the support of the Nevada Cancer Institute which sponsored this research through the NNCI Collaborative Grant Program. Henry Hirschberg is grateful for the support of the Norwegian Radium Hospital Research Foundation. Portions of this work were made possible through access to the Laser Microbeam and Medical Program (LAMMP) and the Chao Cancer Center Optical Biology Shared Resource at the University of California, Irvine.

**Open Access** This article is distributed under the terms of the Creative Commons Attribution Noncommercial License which permits any noncommercial use, distribution, and reproduction in any medium, provided the original author(s) and source are credited.

## References

- Wallner KE, Galicich JH, Krol G, Arbit E, Malkin MG (1989) Patterns of failure following treatment for glioblastoma multiforme and anaplastic astrocytoma. *Int J Radiat Oncol Biol Phys* 16:1405–1409
- Huber J, Egleton R, Davis T (2001) Molecular physiology and pathophysiology of tight junctions in the blood–brain barrier. *Trends Neurosci* 24:719–725. doi:10.1016/S0166-2236(00)02004-X
- Ballabh P, Braun A, Nedergaard M (2004) The blood–brain barrier: an overview: structure, regulation, and clinical implications. *Neurobiol Dis* 16:1–13. doi:10.1016/j.nbd.2003.12.016
- Abbott N, Romero I (1996) Transporting therapeutics across the blood–brain barrier. *Mol Med Today* 2:106–113. doi:10.1016/1357-4310(96)88720-X
- Kemper E, Booger W, Thuis I, Beijnen J, Tellingen O (2004) Modulation of the blood–brain barrier in oncology: therapeutic opportunities for the treatment of brain tumors. *Cancer Treat Rev* 30:415–423. doi:10.1016/j.ctrv.2004.04.001
- Abbott N (2005) Physiology of the blood–brain barrier and its consequences for drug transport to the brain. *Int Congr Ser* 1277:3–18. doi:10.1016/j.ics.2005.02.008
- Pardridge W (2005) The blood–brain barrier: bottleneck in brain drug development. *NeuroRx* 2:3–14. doi:10.1602/neurorx.2.1.3
- Jolliet-Riant P, Tillement JP (1999) Drug transfer across the blood–brain barrier and improvement of brain delivery. *Fundam Clin Pharmacol* 13:16–26
- Doolittle ND, Miner ME, Hall WA, Siegal T, Jerome E, Osztie E, McAllister LD, Bubalo JS, Kraemer DF, Fortin D, Nixon R, Muldoon LL, Neuwelt EA (2000) Safety and efficacy of a multicenter study using intra-arterial chemotherapy in conjunction with osmotic opening of the blood–brain barrier for the treatment of patients with malignant brain tumors. *Cancer* 88(3):637–647. doi:10.1002/(SICI)1097-0142(20000201)88:3<637::AID-CNCR22>3.0.CO;2-Y
- Rand RW, Kreitman RJ, Patronas N, Varricchio F, Pastan I, Puri RK (2000) Intratumoral administration of recombinant circularly permuted interleukin-4-*Pseudomonas* exotoxin in patients with high-grade glioma. *Clin Cancer Res* 6(6):2157–2165
- Sampson JH, Akabani G, Archer GE et al (2003) Progress report of a phase I study of the intracerebral microinfusion of a recombinant chimeric protein composed of transforming growth factor (TGF)-alpha and a mutated form of the *Pseudomonas* exotoxin termed PE-38 (TP-38) for the treatment of malignant brain tumors. *J Neurooncol* 65(1):27–35. doi:10.1023/A:1026290315809
- Bobo RH, Laske DW, Akbasak A, Morrison PF, Dedrick RL, Oldfield EH (1994) Convection-enhanced delivery of macromolecules in the brain. *Proc Natl Acad Sci USA* 91:2076–2080. doi:10.1073/pnas.91.6.2076
- Lieberman DM, Laske DW, Morrison PF, Bankiewicz KS, Oldfield EH (1995) Convection-enhanced distribution of large molecules in gray matter during interstitial drug infusion. *J Neurosurg* 82:1021–1029
- Lidar Z, Mardor Y, Jonas T, Pfeffer R, Faibel M, Hadani M, Ram Z (2004) Convection-enhanced delivery of paclitaxel for the treatment of recurrent glioblastoma. A phase I/II clinical study. *J Neurosurg* 100:472–479
- Brem H, Piantadosi S, Burger PC, Walker M, Selker R, Vick NA, Black KL, Sisti M, Brem S, Mohr G, Muller P, Morawetz R, Schold SC, Polymer-Brain Tumor Treatment Group (1995) Placebo-controlled trial of safety and efficacy of intraoperative controlled delivery by biodegradable polymers of chemotherapy for recurrent gliomas. *Lancet* 345(8956):1008–1012. doi:10.1016/S0140-6736(95)90755-6
- Lawson HC, Sampath P, Bohan E, Park MC, Hussain N, Olivi A, Weingart J, Kleinberg L, Brem H (2007) Interstitial chemotherapy for malignant gliomas: the Johns Hopkins experience. *J Neurooncol* 83(1):61–70. doi:10.1007/s11060-006-9303-1
- Choi JJ, Pernet M, Small SA, Konofagou EE (2007) Noninvasive, transcranial and localized opening of the blood–brain barrier using focused ultrasound in mice. *Ultrasound Med Biol* 33(1):95–104. doi:10.1016/j.ultrasmedbio.2006.07.018
- Treat LH, McDannold N, Vykhodtseva N, Zhang Y, Tam K, Hynynen K (2007) Targeted delivery of doxorubicin to the rat brain at therapeutic levels using MRI-guided focused ultrasound. *Int J Cancer* 121:901–907. doi:10.1002/ijc.22732
- Worthington R, Mulders M (1975) The effect of *Clostridium perfringens* epsilon toxin on the blood brain barrier of mice. *Onderstepoort J Vet Res* 42:25–28
- Nagahama M, Sakurai J (1991) Distribution of labeled *Clostridium perfringens* epsilon toxin in mice. *Toxicon* 29:211–217. doi:10.1016/0041-0101(91)90105-Z
- Dorca-Arévalo J, Soler-Jover A, Gibert M, Popoff M, Martín-Satué M, Blasi J (2008) Binding of epsilon-toxin from *Clostridium perfringens* in the nervous system. *Vet Microbiol* 131:14–25. doi:10.1016/j.vetmic.2008.02.015
- Zhu C, Ghabriel M, Blumbergs P, Reilly P, Manavis J, Youssef J, Hatami S, Finnie J (2001) *Clostridium perfringens* prototoxin-induced alteration of endothelial barrier antigen (EBA)

- immunoreactivity at the blood–brain barrier (BBB). *Exp Neurol* 169:72–82. doi:[10.1006/exnr.2001.7652](https://doi.org/10.1006/exnr.2001.7652)
23. Berg K, Selbo PK, Prasmickaite L, Tjelle TE, Sandvig K, Moan J, Gaudernack G, Fodstad O, Kjølstrud S, Anholt H, Rodal GH, Rodal SK, Høgset A (1999) Photochemical internalization: a novel technology for delivery of macromolecules into cytosol. *Cancer Res* 59:1180–1183
  24. Dietze A, Peng Q, Selbo PK, Kaalhus O, Muller C, Bown S, Berg K (2005) Enhanced photodynamic destruction of a transplantable fibrosarcoma using photochemical internalisation of gelonin. *Br J Cancer* 92:2004–2009. doi:[10.1038/sj.bjc.6602600](https://doi.org/10.1038/sj.bjc.6602600)
  25. Selbo PK, Kaalhus O, Sivam G, Berg K (2001) 5-Aminolevulinic acid-based photochemical internalization of the immunotoxin MOC31-gelonin generates synergistic cytotoxic effects in vitro. *Photochem Photobiol* 74(2):303–310. doi:[10.1562/0031-8655\(2001\)074<0303:AABPIO>2.0.CO;2](https://doi.org/10.1562/0031-8655(2001)074<0303:AABPIO>2.0.CO;2)
  26. Selbo PK, Sivam G, Fodstad Ø, Sandvig K, Berg K (2000) Photochemical internalisation increases the cytotoxic effect of the immunotoxin MOC31-gelonin. *Int J Cancer* 87:853–859. doi:[10.1002/1097-0215\(20000915\)87:6<853::AID-IJC15>3.0.CO;2-0](https://doi.org/10.1002/1097-0215(20000915)87:6<853::AID-IJC15>3.0.CO;2-0)
  27. Prasmickaite L, Høgset A, Selbo P, Engesæter B, Hellum M, Berg K (2002) Photochemical disruption of endocytic vesicles before delivery of drugs: a new strategy for cancer therapy. *Br J Cancer* 86:652–657. doi:[10.1038/sj.bjc.6600138](https://doi.org/10.1038/sj.bjc.6600138)
  28. Hirschberg H, Uzal FA, Chighvinadze D, Zhang MJ, Peng Q, Madsen SJ (2008) Disruption of the blood-brain barrier following ALA-mediated photodynamic therapy. *Lasers Surg Med* 40(8):535–542
  29. Barth RF (1998) Rat brain tumor models in experimental neuro-oncology: the 9L, C6, T9, F98, RG2 (D74), RT-2 and CNS-1 gliomas. *J Neurooncol* 36:91–102. doi:[10.1023/A:1005805203044](https://doi.org/10.1023/A:1005805203044)
  30. Hirschberg H, Sun CH, Krasieva T, Madsen SJ (2006) Effects of ALA-mediated photodynamic therapy on the invasiveness of human glioma cells. *Lasers Surg Med* 38(10):939–945
  31. Michl P, Buchholz M, Rolke M et al (2001) Claudin-4: a new target for pancreatic cancer treatment using *Clostridium perfringens* enterotoxin. *Gastroenterology* 121:678–684. doi:[10.1053/gast.2001.27124](https://doi.org/10.1053/gast.2001.27124)
  32. Kominsky SL, Vali M, Korz D, Gabig TG, Weitzman SA, Argani P, Sukumar S (2004) *Clostridium perfringens* enterotoxin elicits rapid and specific cytolysis of breast carcinoma cells mediated through tight junction proteins claudin 3 and 4. *Am J Pathol* 164(5):1627–1633
  33. Kominsky SL, Tyler B, Sosnowski J, Brady K, Doucet M, Nell D, Smedley JG 3rd, McClane B, Brem H, Sukumar S (2007) *Clostridium perfringens* enterotoxin as a novel-targeted therapeutic for brain metastasis. *Cancer Res* 67(17):7977–7982
  34. Buxton D (1976) Use of horseradish peroxidase to study the antagonism of *Clostridium welchii* (*Cl. perfringens*) type D epsilon toxin in mice by the formalinized epsilon prototoxin. *J Comp Pathol* 86:67–72. doi:[10.1016/0021-9975\(76\)90029-3](https://doi.org/10.1016/0021-9975(76)90029-3)
  35. Fingar VH (1996) Vascular effects of photodynamic therapy. *J Clin Laser Med Surg* 14:323–328
  36. Snyder JW, William R, Greco WR, Bellnier DA, Vaughan L, Henderson BW (2003) Photodynamic therapy: a means to enhanced drug delivery to tumors. *Cancer Res* 63:8126–8131
  37. Barth RF, Yang W, Coderre JA (2003) Rat brain tumor models to assess the efficacy of boron neutron capture therapy: a critical evaluation. *J Neurooncol* 62(1–2):61–74
  38. Giese A, Bjerkvig R, Berens ME, Westphal M (2003) Cost of migration: invasion of malignant gliomas and implications for treatment. *J Clin Oncol* 21(8):1624–1636. doi:[10.1200/JCO.2003.05.063](https://doi.org/10.1200/JCO.2003.05.063)
  39. Madsen SJ, Sun C-H, Tromberg BJ, Hirschberg H (2001) Development of a novel balloon applicator for optimizing light delivery in photodynamic therapy. *Lasers Surg Med* 29:406–412. doi:[10.1002/lsm.10005](https://doi.org/10.1002/lsm.10005)
  40. Inamura T, Nomura T, Bartus RT et al (1994) Intracarotid infusion of RMP-7, a bradykinin analog: a method for selective drug delivery to brain tumors. *J Neurosurg* 81:752–758
  41. Matsukado K, Inamura T, Nakano S et al (1996) Enhanced tumor uptake of carboplatin and survival in glioma-bearing rats by intracarotid infusion of bradykinin analog, RMP-7. *Neurosurgery* 39:125–133. doi:[10.1097/00006123-199607000-00025](https://doi.org/10.1097/00006123-199607000-00025)
  42. Matsukado K, Sugita M, Black K (1998) Intracarotid low dose bradykinin infusion selectively increases tumor permeability through activation of bradykinin B2 receptors in malignant gliomas. *Brain Res* 792:10–15. doi:[10.1016/S0006-8993\(97\)01502-3](https://doi.org/10.1016/S0006-8993(97)01502-3)